

# Experimentally Motivated Order of Length Scales Affect Shot Noise

Sourav Manna<sup>1,2,\*</sup> and Ankur Das<sup>1,†</sup>

<sup>1</sup>*Department of Condensed Matter Physics, Weizmann Institute of Science, Rehovot 7610001, Israel*

<sup>2</sup>*Raymond and Beverly Sackler School of Physics and Astronomy, Tel-Aviv University, Tel Aviv 6997801, Israel*

Shot noise at a conductance plateau in a quantum point contact (QPC) can be explained by considering equilibrations at the quantum Hall edges. The indication from recent experiments is that the charge equilibration length is much shorter than the thermal equilibration length. We discuss how this discovery gives rise to different thermal equilibration regimes in the presence of full charge equilibration. In this work, we classify these distinct regimes via dc current-current correlations (*electrical shot noise*) at distinct QPC conductance plateaus for the edges of integer, particle-like, and hole-like filling fractions in a two dimensional electron gas.

## I. INTRODUCTION

Quantum Hall effect is one of the oldest known phenomena that requires understanding of band topology and quantum mechanics [1–5]. However, the bulk-boundary correspondence [6] does not guarantee a comprehensive understanding of the edges for a given bulk topological order. Thus, we can separate our question of the quantum Hall effect into two different pieces : (1) the topological order of the bulk and (2) the details (for example the steady state) of the edge. There is more than one known mechanism that can make the picture of the edge fuzzy keeping the bulk-boundary correspondence intact.

One of the phenomena that plagued the quantum Hall edge theory is the edge reconstruction. This is an umbrella term that includes the appearance of new counter-propagating modes [7–9], reordering of the edge modes [10], emergence of an effective narrow strip of spin rotation [11], and more. This was first discussed for the two dimensional electron gas (2DEG) by Chamon and Wen [12] almost three decades ago. They explained how the sharpness of the confining potential can cause the appearance of new counter-propagating edge modes. Following this, there have been numerous efforts to understand the edge reconstruction for integer and fractional quantum Hall systems [13]. More recently, we have learned that even integer quantum Hall edges can have a fractional edge reconstruction [8]. The general answer to the question of when and how edge reconstruction takes place is a non-universal one. This makes the study of edge reconstruction a difficult and detailed topic of interest for both the experimentalists and theorists.

Typically in an experiment, a dc voltage is used as the source which causes voltage drops near different contacts. This gives rise to the Joule heating which produces heat and the heating effects can play a crucial role in the edge transport. Heat, which propagates along the edge modes, induces particle-hole pairs and thermally activates the tunneling of particles and holes among the

edge modes. This gives rise to a remarkable phenomenon known as the edge equilibration [14–21]. Such an incoherent phenomenon leads the steady state of edges to a hydrodynamic regime and the edge modes are equilibrated to a hydrodynamic mode of a given chirality. Such a mode is characterized by its electrical and thermal conductances. Tunneling of particles and holes allows the exchange of both charge and heat. This leads to the electro-chemical potential and thermal equilibrations, respectively [14, 19, 20]. The particle-hole pairs can split stochastically into two modes and move into opposite directions in the case of the edges comprising of counter-propagating modes. This mechanism gives rise to the electrical shot noise (current-current correlations), which provides a fully electrical approach to capture the effect of heat propagation along the edges.

In electrical current, there can be fluctuations due to the stochastic injection of particles or holes. Now, the topological properties of a quantum Hall edge allows only certain types of quasi-particle tunnelings to take place, which in turn allows the measurement of quasi-particle charge. Quantum point contact (QPC), described below (c.f. Fig. 1), is one of the ways to generate this stochastic tunneling. However, this is not the only mechanism that can generate shot noise. For example, the decay of neutralons (quanta of the neutral modes) can be one of those mechanisms [22, 23]. We will discuss another mechanism due to the equilibration later.

Now, the natural question will be how to poke the properties of the edge modes beyond the topological charge and thermal conductances. One of the established techniques is to push the opposite edges of a quantum Hall system close to each other so that they start to tunnel. This is done by an electrostatic constriction, namely a QPC. In the context of the quantum Hall effect, QPC plays a pivotal role in understanding the microscopic structure of the edge. There are at least two types of measurements one can do in a QPC device : (1) transport and (2) shot noise. As the QPC constriction gets narrower, less current will transmit across the QPC. Now one question can be asked if we find that the transmission remains constant (leading to a transmission plateau) as we make the constriction narrower [24, 25]. In that case, there can be at least two possible scenarios : (1) there

\* [sourav.manna@weizmann.ac.il](mailto:sourav.manna@weizmann.ac.il)

† [ankur.das@weizmann.ac.il](mailto:ankur.das@weizmann.ac.il)

are more than one coherently propagating edge modes, and a few of them completely backscatter, while the others fully transmit across the QPC and (2) at the QPC constriction, a very small region of a quantum Hall liquid of a different filling fraction is stabilized such that when these modes electrically equilibrate (incoherent regime), it leads to a transmission plateau. We can also ask if there are shot noise signatures of these scenarios other than the transport measurements.

In recent times, there have been immense development in QPC and sample standardizations and we have learned that we must treat the equilibration scenario more carefully. What we have learned is that there are *two different* internal length scales involved here, namely the electro-chemical potential or charge equilibration length ( $l_{\text{eq}}^{\text{ch}}$ ) and the thermal equilibration length ( $l_{\text{eq}}^{\text{th}}$ ). Recent experiments have demonstrated that they are not the same order of magnitude [26–28]. There are two geometric length scales in a QPC geometry (c.f. Fig. 1): (1) length of the arms ( $L_A$ ) and (2) size of the QPC ( $L_Q$ ). We know that  $L_A \gg L_Q$  and from the experiments [26–28] we have  $l_{\text{eq}}^{\text{ch}} \ll l_{\text{eq}}^{\text{th}}$ . To have a transmission plateau we must have  $l_{\text{eq}}^{\text{ch}} \ll (L_A, L_Q)$  leading to the full charge equilibration in every segment of the QPC geometry. However, the degree of thermal equilibration can be in a distinct regime in different segments. Thus, the interplay among the order of magnitudes of  $l_{\text{eq}}^{\text{th}}$ ,  $L_A$ ,  $L_Q$  leads to distinct inequalities giving rise to a zoo of scenarios. We study the effect of these inequalities in the electrical shot noise (defined below).

We refer to Fig. 1 for a schematic picture of the QPC geometry and the corresponding transport and shot noise measurements. We have  $I_1$  and  $I_2$  as the currents which enter the drains  $D_1$  and  $D_2$ , respectively. We define the dc current-current auto-correlations as  $\delta^2 I_1$  in  $D_1$ ,  $\delta^2 I_2$  in  $D_2$ , and the cross-correlation as  $\delta^2 I_c$  [29] where

$$\begin{aligned} \delta^2 I_1 &= \langle (I_1 - \langle I_1 \rangle)^2 \rangle, \\ \delta^2 I_2 &= \langle (I_2 - \langle I_2 \rangle)^2 \rangle, \\ \delta^2 I_c &= \langle (I_1 - \langle I_1 \rangle) (I_2 - \langle I_2 \rangle) \rangle. \end{aligned} \quad (1)$$

The shot noise Fano factors are defined as

$$F_j = \frac{\delta^2 I_j}{2eI_S t(1-t)}, \quad j \in \{1, 2, c\} \quad (2)$$

where  $I_S$  is the source current and  $t = I_1/I_S$  is the QPC transmission.

In the following sections, we describe the keynote points of our work (Section II), the assumptions and techniques we use (Section III), and our insight into the results (Section IV). We draw a summary and the future prospect of our work in Section V.

## II. KEYNOTE POINTS

Being motivated by the experiments [25, 30] and previously studied cases [18, 31, 32], we analyze the effects

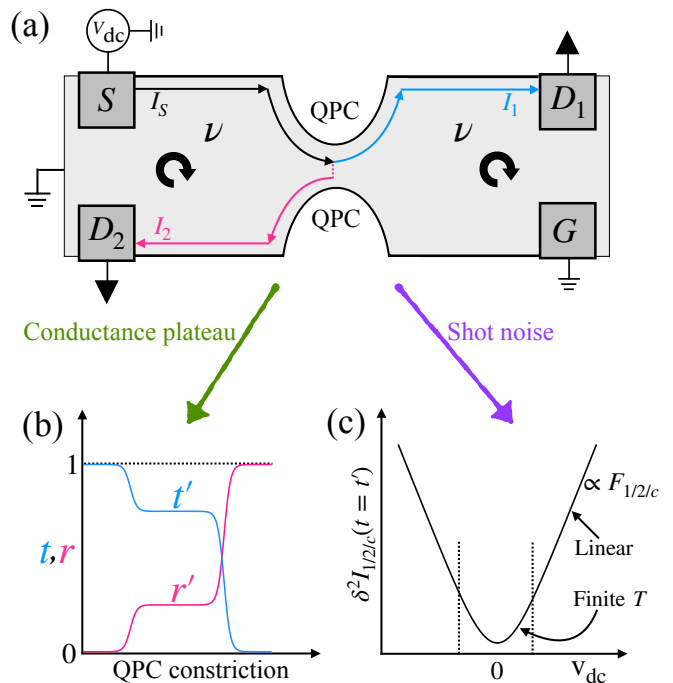


FIG. 1. A schematic picture of the device and measurements, which we use throughout the paper. (a) We show a Hall bar with filling  $\nu$  in a QPC geometry. We have four contacts as a source  $S$ , a ground  $G$ , and two drains  $D_1, D_2$ . A dc current  $I_S$  is injected by  $S$ , which is biased by a dc voltage  $V_{\text{dc}}$ , and the measurements are performed at  $D_1, D_2$ . We describe the chirality of charge propagation by circular arrows. (b) Transport measurements are carried out by measuring currents  $I_1, I_2$  at  $D_1, D_2$  respectively. The transmission and reflection coefficients are  $t = I_1/I_S$  and  $r = I_2/I_S$  respectively, where  $t+r = 1$ . A QPC transmission plateau can be observed at a transmission  $t = t'$  while measuring  $t$  (correspondingly  $r$ ) as a function of the QPC constriction (from a fully open to a fully pinched off QPC). (c) At a transmission plateau ( $t = t'$ ), the current reaching  $D_1, D_2$  can be noisy (leading to  $\delta^2 I_{1/2/c}(t = t') \neq 0$ ) and there can be different mechanisms to it. The functional dependence of  $\delta^2 I_{1/2/c}(t = t')$  is schematically shown while changing  $V_{\text{dc}}$  and the slope of the linear region is proportional to the corresponding Fano factor  $F_{1/2/c}$ . The curvature in  $\delta^2 I_{1/2/c}(t = t')$  shows up due to the temperature dependence.

of different orders of length scales on the shot noise signatures and compare the corresponding different Fano factors in full completeness. Here, we not only do a qualitative analysis but also calculate the quantitative values of the Fano factors for all the cases considering the inequalities among  $l_{\text{eq}}^{\text{ch}}$ ,  $l_{\text{eq}}^{\text{th}}$ ,  $L_A$ ,  $L_Q$ . As we do not have any control over the internal length scales, we consider different reasonable scenarios.

1. In these results (c.f. Table I), we find interesting structures in the Fano factors for different regimes. We find that the  $\nu = \text{particle-like}$  and  $\nu = \text{hole-like}$  states (c.f. Table II) behave *differently* in their shot noise signatures.

$\nu$	$\nu_i$	No equilibration ( $F_1 = F_2, F_c$ )	Mixed equilibration ( $F_1 = F_2, F_c$ )	Full equilibration ( $F_1 = F_2, F_c$ )
1	1/3	$\approx (0.36, -0.36)$	$\approx (0.36, -0.36)$	$\approx (0.55\sqrt{l_{\text{eq}}^{\text{th}}/L_Q}, -0.55\sqrt{l_{\text{eq}}^{\text{th}}/L_Q})$
	2/3	$\approx (0.33, -0.33)$	$\approx (0.33, -0.33)$	$\approx (0.55\sqrt{l_{\text{eq}}^{\text{th}}/L_Q}, -0.55\sqrt{l_{\text{eq}}^{\text{th}}/L_Q})$
2/5	1/3	$\approx (0.1, -0.1)$	$\approx (0.1, -0.1)$	$\approx (0.0, -0.0)$
3/7	1/3	$\approx (0.086, -0.086)$	$\approx (0.086, -0.086)$	$\approx (0.0, -0.0)$
	2/5	$\approx (0.066, -0.066)$	$\approx (0.066, -0.066)$	$\approx (0.0, -0.0)$
2/3	1/3	$\approx (0.35, -0.22)$	$\approx (0.09 + 0.3\sqrt{L_A/l_{\text{eq}}^{\text{th}}}, 0.09 - 0.3\sqrt{L_A/l_{\text{eq}}^{\text{th}}})$	$\approx (0.09 + 0.3\sqrt{L_A/l_{\text{eq}}^{\text{th}}}, 0.09 - 0.3\sqrt{L_A/l_{\text{eq}}^{\text{th}}})$
	[1/3]	$\approx (0.28, -0.1)$	$\approx (0.09 + 0.3\sqrt{L_A/l_{\text{eq}}^{\text{th}}}, 0.09 - 0.3\sqrt{L_A/l_{\text{eq}}^{\text{th}}})$	$\approx (0.09 + 0.3\sqrt{L_A/l_{\text{eq}}^{\text{th}}}, 0.09 - 0.3\sqrt{L_A/l_{\text{eq}}^{\text{th}}})$
3/5	1/3	$\approx (0.37, -0.097)$	$\approx (0.52, -0.31)$	$\approx (0.52, -0.31)$
	2/5	$\approx (0.38, -0.09)$	$\approx (0.52, -0.3)$	$\approx (0.52, -0.3)$
4/7	1/3	$\approx (0.39, -0.009)$	$\approx (0.39, -0.19)$	$\approx (0.39, -0.19)$
	2/5	$\approx (0.43, -0.009)$	$\approx (0.38, -0.18)$	$\approx (0.38, -0.18)$
	3/7	$\approx (0.45, -0.008)$	$\approx (0.38, -0.16)$	$\approx (0.38, -0.16)$

TABLE I. Summary of our shot noise results :  $F_1, F_2$  are the auto-correlation Fano factors for the drains  $D_1, D_2$ , respectively, while  $F_c$  is the cross-correlation Fano factor for different bulk filling factor  $\nu$  and QPC filling factor  $\nu_i$  in distinct thermal equilibration regimes namely “No”, “Mixed”, and “Full”. We assume full charge equilibration and different degree of thermal equilibration in each of the segments  $L_A, L_Q$  (c.f. Fig. 2). We always have  $F_1 = F_2$ , but  $F_c$  is not always equal in magnitude to  $F_1 = F_2$ . For the  $\nu =$  particle-like states, “Mixed” and “No” thermal equilibrations have the same values for  $F_1 = F_2$  and  $F_c$  (shaded pink) for a given  $\{\nu, \nu_i\}$ . Similarly, for the  $\nu =$  hole-like states we find that  $F_1 = F_2$  and  $F_c$  acquire the same values for “Mixed” and “Full” thermal equilibrations (shaded blue) for a given  $\{\nu, \nu_i\}$ . Here,  $l_{\text{eq}}^{\text{th}}$  denotes the thermal equilibration length and  $\approx 0$  indicating an exponential suppression as a function of the geometric lengths. We mention that  $\{\nu, \nu_i\} = \{2/3, [1/3]\}$  denotes the 1/3 edge reconstruction in  $\nu = 2/3$  [7] and the results for  $\nu = 2/3$  also appear in [31, 32].

- Namely, the Fano factor values for the  $\nu =$  particle-like states are the same for the “No” and “Mixed” thermal equilibrations (arms are thermally equilibrated while edges around the QPC are not thermally equilibrated) for a given  $\{\nu, \nu_i\}$ . This is because all the modes are co-propagating, and equilibrating those in the arm (“outer” segment) does not make a difference (c.f. Fig. 3(a)).
- However, the situation changes for the  $\nu =$  hole-like states where the Fano factors for the “Mixed” and “Full” thermal equilibrations are equal for a given  $\{\nu, \nu_i\}$ . This is because the counter-propagating modes in the arm (“outer” segment) make sure that all the heat from a hot spot reaches the noise spots for both the “Mixed” and “Full” thermal equilibration regimes (c.f. Fig. 3(b)).
- The Fano factors can be exponentially suppressed (as a function of the geometric lengths) or constant or length dependent depending on the nature of heat transport (ballistic or antiballistic or diffusive, respectively) in different segments of the QPC geometry.
- We also find that for all the  $\nu =$  hole-like states, the auto- and the cross-correlation Fano factors are *not equal*. Though it is not expected from the conventional picture of the shot noise at a QPC geometry but can be understood in the equilibration picture.
- This work provides a comprehensive study, as summarized in Table I, of the shot noise Fano factors

where (1) we take the order of internal lengths  $l_{\text{eq}}^{\text{ch}}, l_{\text{eq}}^{\text{th}}$  seriously including their comparison with the geometric lengths  $L_A, L_Q$  and (2) we find qualitative inequalities for the different Fano factors (besides quantitative values) resolving distinct scenarios.

### III. ASSUMPTIONS AND TECHNIQUES

Taking into considerations the recent experiments [26–28], showing that the thermal equilibration length is order of magnitude larger than the charge equilibration length, and the typical geometric lengths of a QPC geometry (where arm length is much larger than the QPC size) we believe and consider the following three distinct relevant possibilities (c.f. Fig. 2) :

- $l_{\text{eq}}^{\text{th}} \ll L_Q \ll L_A$  : “Full” thermal equilibration regime, where the system is fully thermally equilibrated in every segment.
- $L_Q \ll l_{\text{eq}}^{\text{th}} \ll L_A$  : “Mixed” thermal equilibration regime, where the system is fully thermally equilibrated at the arms but thermally unequilibrated around the QPC.
- $L_Q \ll L_A \ll l_{\text{eq}}^{\text{th}}$  : “No” thermal equilibration regime, where the system is not thermally equilibrated in any segment.

We will focus our analysis on these aforementioned cases and assume  $l_{\text{eq}}^{\text{ch}} \ll (L_A, L_Q)$  providing full charge equilibration in each segment of the QPC geometry.

We use Refs. 18, 20, 31, and 32 and write the general expressions for the auto- and cross-correlations in a QPC geometry for the bulk filling  $\nu$  and QPC filling  $\nu_i$  when  $\nu > \nu_i$  (Fig. 2 and Fig. 3). Charge is assumed to be fully equilibrated, leading to a ballistic charge transport, moving “downstream” along each segment of the QPC geometry. We define antiballistic as the direction opposite to the charge flow (“upstream”). We use those expressions to compute the correlation values for various choices of  $\{\nu, \nu_i\}$  and for different thermal equilibration regimes under considerations assuming no bulk-leakage [15, 17, 33, 34]. We write the  $\delta^2 I_1$ ,  $\delta^2 I_2$ , and  $\delta^2 I_c$  as

$$\delta^2 I_1 = 2 \left( \frac{e^2}{h} \right) \frac{\nu_i}{\nu} (\nu - \nu_i) k_B (T_M + T_N) + \frac{1}{\nu^2} \left[ \nu_i^2 \langle (\Delta I_S)^2 \rangle + (\nu - \nu_i)^2 \langle (\Delta I_G)^2 \rangle \right], \quad (3)$$

$$\delta^2 I_2 = 2 \left( \frac{e^2}{h} \right) \frac{\nu_i}{\nu} (\nu - \nu_i) k_B (T_M + T_N) + \frac{1}{\nu^2} \left[ \nu_i^2 \langle (\Delta I_G)^2 \rangle + (\nu - \nu_i)^2 \langle (\Delta I_S)^2 \rangle \right], \quad (4)$$

$$\delta^2 I_c = -2 \left( \frac{e^2}{h} \right) \frac{\nu_i}{\nu} (\nu - \nu_i) k_B (T_M + T_N) + \frac{\nu_i (\nu - \nu_i)}{\nu^2} \left[ \langle (\Delta I_G)^2 \rangle + \langle (\Delta I_S)^2 \rangle \right], \quad (5)$$

where  $T_M, T_N$  are the temperatures at the noise spots  $M$  and  $N$ , respectively. The corresponding Fano factors can be found by using Eq. (2). We find  $T_M, T_N$  by solving self-consistent equilibration equations and considering energy conservations [18, 20, 31, 32]. Owing to the Joule heating, power is dissipated at the hot spots as

$$P_{H_1} = P_{H_2} = \frac{e^2 V_{dc}^2 \nu_i (\nu - \nu_i)}{h 2\nu}. \quad (6)$$

We compute the contributions  $\langle (\Delta I_G)^2 \rangle = \langle (\Delta I_S)^2 \rangle$  at the noise spots  $O$  and  $P$  by evaluating the following integral ([18, 20]) as

$$\begin{aligned} \langle (\Delta I_S)^2 \rangle &= \langle (\Delta I_G)^2 \rangle \\ &= \frac{2e^2}{h l_{eq}^{ch}} \nu \frac{\nu_-}{\nu_+} \int_0^{L_A} dx \frac{e^{-\frac{2x}{l_{eq}^{ch}}} k_B [T_+(x) + T_-(x)]}{[1 - (e^{-\frac{-L_A}{l_{eq}^{ch}}} \frac{\nu_-}{\nu_+})]^2}, \end{aligned} \quad (7)$$

where  $l_{eq}^{ch}$  is the charge equilibration length and  $\nu = (\nu_+ - \nu_-)$ . We have  $\nu_+$  and  $\nu_-$  as the filling factors of the downstream and upstream modes, respectively. Here  $T_{\pm}(x)$  are the temperature profiles of the modes with filling factors  $\nu_{\pm}$ , respectively. We note that  $T_{\pm}(x)$  depend on the  $l_{eq}^{th}$  and we find these by following Ref. 20. We

$\nu$	Edge structure	$\nu$	Edge structure
1	$\nu = 0$ $\nu = 1$	2/3	(a) $\nu = 0$ $\nu = 2/3$ (b) $\nu = 0$ $\nu = 2/3$ $1/3$ $1/3$ $1/3$
2/5	$\nu = 0$ $\nu = 2/5$	3/5	$\nu = 0$ $\nu = 3/5$ $1/3$ $1/15$
3/7	$\nu = 0$ $\nu = 3/7$	4/7	$\nu = 0$ $\nu = 4/7$ $1/3$ $1/15$ $1/35$

TABLE II. We show the edge structures of integer ( $\nu = 1$ ), particle-like ( $\nu = 1/3, 2/5, 3/7$ ), and hole-like ( $\nu = 2/3, 3/5, 4/7$ ) filling fractions under considerations. Integer and fractional charge modes are depicted as double and single-headed arrows respectively. Each arrow-head shows the chirality of charge propagation of that mode and  $\nu = 0$  corresponds to the vacuum. For  $\nu = 2/3$ , we show the bare edge mode structure in (a) and the  $1/3$  edge reconstruction (blue) [7] in (b).

assume that no voltage drops occur along the “outer” segment (Fig. 3) and

$$T_+(0) = 0, \quad T_-(L_A) = T_M \quad (8)$$

serve as the boundary conditions since we consider that the lead contacts are at zero temperature.

#### IV. INSIGHT INTO THE RESULTS

By looking at the Table I, we find a number of interesting features in the shot noise Fano factors. In the following, we explain those qualitatively :

##### 1. $F_1$ vs. $F_2$ vs. $F_c$ :

- (A)  $F_1 = F_2$  : Two auto-correlations are the same due to the current conservation.
- (B)  $F_c < 0$  : A particle or hole can end up in either  $\bar{D}_1$  or  $D_2$ , which keeps those drains to be anti-correlated, leading to a negative cross-correlation.
- (C)  $F_1 = F_2 \stackrel{?}{=} -F_c$  : We can write Eqs. (3) to (5) in a more simplified manner as  $F_1 = F_2 = F_M + F_N + F_O + F_P$  and  $F_c = -F_M - F_N + F'_O + F'_P$ . If  $\langle (\Delta I_S)^2 \rangle = \langle (\Delta I_G)^2 \rangle \approx 0$ , then we have  $F_O = F_P = F'_O = F'_P \approx 0$  leading to  $F_1 = F_2 = -F_c$ . This equality occurs for the  $\nu =$  particle-like states as they contains co-propagating edges in the “outer” segments. Therefore, heat propagates only ballistically there which leads to the exponentially

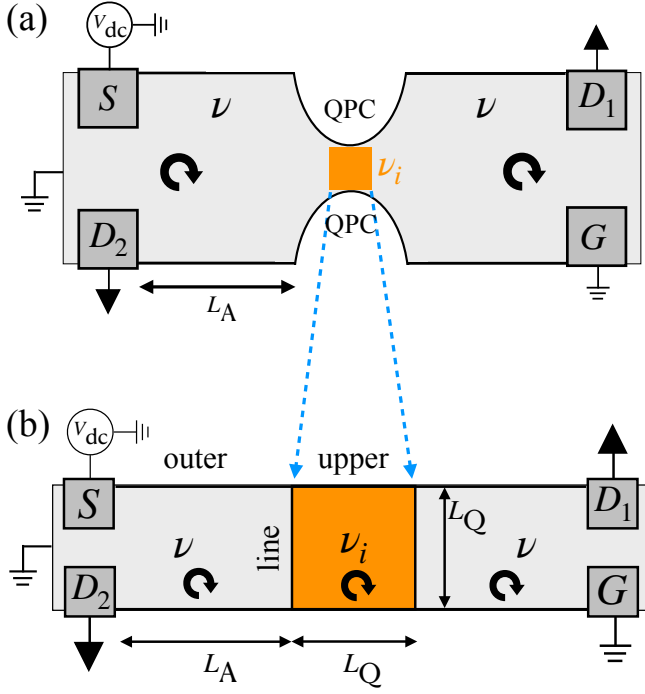


FIG. 2. An effective modeling of the QPC geometry (c.f. Fig. 1(a)) while we consider equilibration. We describe the chirality of charge propagation of each filling by the circular arrows. (a) We schematically show the QPC geometry, where  $\nu$  and  $\nu_i$  are the bulk and QPC filling factors respectively and  $L_A, L_Q$  are the geometric lengths with  $L_Q \ll L_A$ . (b) Effective model of the QPC geometry with edge equilibration for bulk filling  $\nu$  and QPC filling  $\nu_i$ . We show three distinct boundaries: the boundary of  $\nu$  with vacuum as “outer”, the boundary of  $\nu_i$  with vacuum as “upper”, and the boundary between  $\nu$  and  $\nu_i$  as “line”.

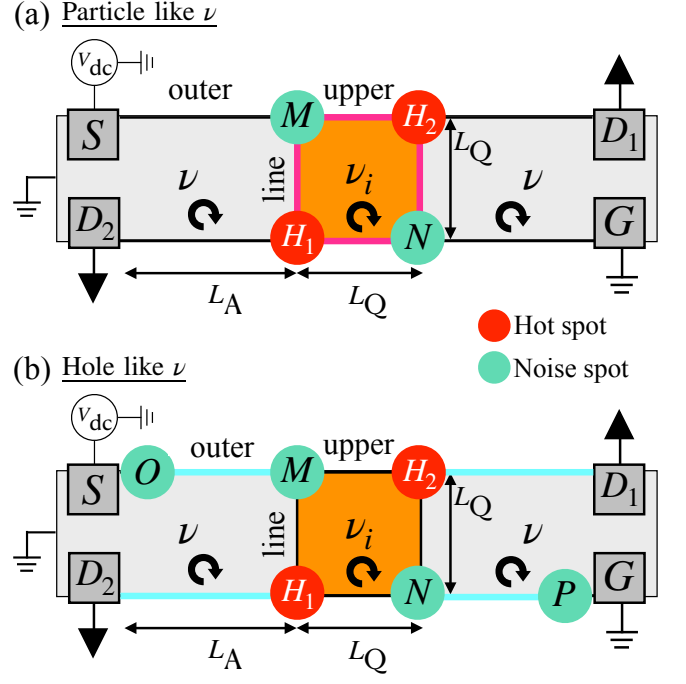
suppressed contributions from the  $O, P$  noise spots (Fig. 3(a)).

On the contrary, for the  $\nu =$  hole-like states we have counter-propagating edge modes in the “outer” segments. Therefore, heat can also propagate diffusively or antiballistically there which lead to constant contributions from the  $O, P$  noise spots as  $\langle(\Delta I_S)^2\rangle = \langle(\Delta I_G)^2\rangle \neq 0$  (Fig. 3(b)). This leads to each of the  $F_O, F_P, F'_O, F'_P$  to be  $\neq 0$  and hence  $F_1 = F_2 \neq -F_c$ .

2.  $F_1 = F_2 = -F_c \approx 0$  :

If we have ballistic heat propagation along each of the “outer”, “line”, and “upper” segments, then heat can not reach efficiently from any hot spot to any noise spot. This leads to an exponentially suppressed contribution to the shot noise from each noise spot. Thereby,  $F_M = F_N = F_O = F_P = F'_O = F'_P \approx 0$  leading to  $F_1 = F_2 = -F_c \approx 0$ .

3.  $(F_1 = F_2, F_c) = \text{constant or } f(l_{\text{eq}}^{\text{th}}, L_Q, L_A)$  :



$\nu$	outer	line	upper
Particle like	B	B/D/AB	B/D/AB
Hole like	B/D/AB	B/AB	B

FIG. 3. We show the generation of hotspots (red circles) resulting in noise spots (green circles) while considering the equilibration for both the  $\nu =$  particle-like and  $\nu =$  hole-like filling fractions. The chirality of charge propagation of each filling is depicted by the circular arrows. (a) We have  $\nu$  as the particle-like filling fraction. The nature of heat transport is ballistic (“B”) in the “outer” segment and can be “B” or diffusive (“D”) or anti-ballistic (“AB”) in the “line” and “upper” segments. We have two hot spots as  $H_1, H_2$ , which result in two noise spots as  $M, N$ . We note that the nature of heat transport in the “line” and “upper” segments (pink shaded lines) determine whether we have a constant noise or length-dependent noise. (b) We have  $\nu$  as the hole-like filling fraction. The nature of heat transport can be “B” or “D” or “AB” in the “outer” segment, can be “B” or “AB” in the “line” segment, and is “B” in the “upper” segment. We have two hot spots as  $H_1, H_2$ , which result in four noise spots as  $M, N, O, P$ . As there can be “D” or “AB” heat transport in the “outer” segment, hence we have additional noise spots  $O, P$ . We note that the nature of heat transport in the “outer” segment (blue shaded lines) determine whether we have a constant noise or a length-dependent noise.

If we have only ballistic and antiballistic heat transports along each of the segments of the QPC geometry, then heat can reach from any hot spot to any noise spot inefficiently or efficiently, respectively. Thereby, a zero or constant contribution to the shot noise Fano factors can be attributed.

However, if the heat is transported diffusively

through any segment then it reaches to the contacts very slowly along that segment. This gives rise to a length dependence in the temperatures of the hot spots. The length dependence has a functional form relating the geometric length of that segment and  $l_{\text{eq}}^{\text{th}}$ . The heat reaches from the hot spots to the noise spots and thus the noise spots also acquire that length scale dependence in their temperatures, which is manifested in the shot noises. From Table I we note that we have diffusive heat transports for  $\{1, 1/3\}$  and  $\{1, 2/3\}$  along “line” and “upper” segments respectively leading to a  $\sqrt{l_{\text{eq}}^{\text{th}}/L_Q}$  dependence in the Fano factors. Similarly, for  $\{2/3, 1/3\}$  and  $\{2/3, [1/3]\}$  diffusive heat transports occur along the “outer” segment leading to a  $\sqrt{L_A/l_{\text{eq}}^{\text{th}}}$  dependence in the Fano factors.

4. “No” = “Mixed”  $\neq$  “Full” for  $\nu$  = particle-like :

The difference between “No” and “Mixed” thermal equilibration regimes is that all the edge modes remain thermally unequilibrated in the former while they equilibrate in the latter only along the “outer” segment (c.f. Fig. 3(a)). Now, for the  $\nu$  = particle-like states the heat transport along the “outer” segment is ballistic always since we have co-propagating modes. Hence, it does not matter if those modes in the “outer” segment thermally equilibrate or not, since they will not contribute to the shot noise leading to “No” = “Mixed”. However, in the “Full” thermal equilibration regime the modes thermally equilibrate both along the “line” and “upper” segments (c.f. Fig. 3(a)) leading to “No” = “Mixed”  $\neq$  “Full”.

5. “No”  $\neq$  “Mixed” = “Full” for  $\nu$  = hole-like :

A common fact between the “Mixed” and “Full” thermal equilibration regimes is that the “outer” segment is thermally equilibrated for both and the heat transport along the “outer” segment is antiballistic (c.f. Fig. 3(b)). Therefore, no heat can reach to the drains from a hot spot. It does not matter if the “line” and “upper” segments (c.f. Fig. 3(b)) are thermally equilibrated (“Full”) or not (“Mixed”), all the heat is transferred from a hot spot to the noise spots leading to “Mixed” = “Full”. However, in the “No” thermal equilibration regime the modes are not thermally equilibrated along the “outer” segment. Hence the ballistic modes, connecting a hot spot to its nearest drain, leak some amount of heat to that drain leading to “No”  $\neq$  “Mixed” = “Full”.

## V. SUMMARY AND FUTURE PROSPECTS

In this work, we have shown how the latest findings [26–28] of the inequality between charge and thermal

equilibration lengths can affect the electrical shot noise. We have analyzed different Abelian quantum Hall states as the bulk filling ( $\nu$ ) and their known or possible QPC transmission plateaus (Table II). We have assumed full charge equilibration throughout our analysis, which has licensed us in determining the transmission plateau for a given QPC filling ( $\nu_i$ ). We have considered three different inequalities among the geometric lengths ( $L_A, L_Q$ ) and the thermal equilibration lengths ( $l_{\text{eq}}^{\text{th}}$ ). These three regimes of thermal equilibration have been denoted as “No” (both the arm and the edges around QPC are thermally unequilibrated), “Mixed” (the arm is thermally equilibrated but not the edges around QPC), and “Full” (both the arm and the edges around QPC are thermally equilibrated). We have found for the  $\nu$  = particle-like states the thermal equilibration of the edges around the QPC affects the shot noise and for the  $\nu$  = hole-like states the thermal equilibration of the edges at the arms affects the shot noise (c.f. Table I and Fig. 3). We have found that the magnitude of the auto-correlation Fano factors is always larger than the cross-correlation Fano factor for the hole-like states, since the thermal transport contribution along the arm is either diffusive or antiballistic.

This work is a step in understanding how the shot noise is affected by different thermal equilibration regimes in a QPC geometry at a QPC transmission plateau. We note that the analyses are valid if we consider similar geometry made out of interfaces [18]. This work can be extended beyond the Abelian quantum Hall states to the non-Abelian fillings (e.g.  $\nu = 12/5$  [35, 36]), where there are no extensive studies yet (recently  $\nu = 5/2$  is considered [18]). In this work, we only focus on understanding the conventional QPC transmission plateau without the engineered interface modes. However, 2DEG interface QPC [37] is an intriguing direction that we hope to look into in the future. Another interesting direction will be the graphene quantum Hall effect. With the recent improvements and understandings, QPC and interfaces in graphene quantum Hall systems have become very relevant [38, 39]. We also note that in graphene how to construct a QPC is not unique, which makes the problem even richer. Interesting future directions may include other topological insulators (for example quantum spin Hall states) [11, 40, 41], quantum spin liquids [42–44], and more.

A recent work Ref. 45 has also discussed the auto- and cross-correlation shot noise.

## ACKNOWLEDGMENTS

We thank Moshe Goldstein and Yuval Gefen for many illuminating discussions and collaboration on related works. We thank Udit Khanna for useful discussions. S.M. was supported by the Weizmann Institute of Science, Israel Deans fellowship through Feinberg Graduate School, as well as the Raymond Beverly Sackler Center for Computational Molecular and Material Science at Tel

Aviv University. A.D. was supported by the German-Israeli Foundation Grant No. I-1505-303.10/2019, DFG MI 658/10-2, DFG RO 2247/11-1, DFG EG 96/13-1, and CRC 183 (project C01). A.D. also thanks the Israel Plan-

ning and budgeting committee (PBC) and the Weizmann Institute of Science, the Dean of Faculty fellowship, and the Koshland Foundation for financial support.

- 
- [1] D. C. Tsui, H. L. Stormer, and A. C. Gossard, Two-dimensional magnetotransport in the extreme quantum limit, *Phys. Rev. Lett.* **48**, 1559 (1982).
- [2] R. B. Laughlin, Anomalous quantum hall effect: An incompressible quantum fluid with fractionally charged excitations, *Phys. Rev. Lett.* **50**, 1395 (1983).
- [3] M. Z. Hasan and C. L. Kane, Colloquium: Topological insulators, *Rev. Mod. Phys.* **82**, 3045 (2010).
- [4] T. H. Hansson, M. Hermanns, S. H. Simon, and S. F. Viefers, Quantum hall physics: Hierarchies and conformal field theory techniques, *Rev. Mod. Phys.* **89**, 025005 (2017).
- [5] C.-Z. Chang, C.-X. Liu, and A. H. MacDonald, Colloquium: Quantum anomalous hall effect, *Rev. Mod. Phys.* **95**, 011002 (2023).
- [6] X. G. Wen, Gapless boundary excitations in the quantum hall states and in the chiral spin states, *Phys. Rev. B* **43**, 11025 (1991).
- [7] J. Wang, Y. Meir, and Y. Gefen, Edge reconstruction in the  $\nu=2/3$  fractional quantum hall state, *Phys. Rev. Lett.* **111**, 246803 (2013).
- [8] U. Khanna, M. Goldstein, and Y. Gefen, Fractional edge reconstruction in integer quantum hall phases, *Phys. Rev. B* **103**, L121302 (2021).
- [9] U. Khanna, M. Goldstein, and Y. Gefen, Emergence of neutral modes in Laughlin-like fractional quantum hall phases, *Phys. Rev. Lett.* **129**, 146801 (2022).
- [10] U. Khanna, G. Murthy, S. Rao, and Y. Gefen, Spin mode switching at the edge of a quantum hall system, *Phys. Rev. Lett.* **119**, 186804 (2017).
- [11] U. Khanna, Y. Gefen, O. Entin-Wohlman, and A. Aharony, Edge reconstruction of a time-reversal invariant insulator: Compressible-incompressible stripes, *Phys. Rev. Lett.* **128**, 186801 (2022).
- [12] C. d. C. Chamon and X. G. Wen, Sharp and smooth boundaries of quantum hall liquids, *Phys. Rev. B* **49**, 8227 (1994).
- [13] U. Khanna, M. Goldstein, and Y. Gefen, Edge reconstruction and emergent neutral modes in integer and fractional quantum hall phases, *Low Temperature Physics* **48**, 420 (2022).
- [14] I. Protopopov, Y. Gefen, and A. Mirlin, Transport in a disordered  $\nu = 2/3$  fractional quantum hall junction, *Annals of Physics* **385**, 287 (2017).
- [15] C. Spånslätt, J. Park, Y. Gefen, and A. D. Mirlin, Topological classification of shot noise on fractional quantum hall edges, *Phys. Rev. Lett.* **123**, 137701 (2019).
- [16] J. Park, A. D. Mirlin, B. Rosenow, and Y. Gefen, Noise on complex quantum hall edges: Chiral anomaly and heat diffusion, *Phys. Rev. B* **99**, 161302 (2019).
- [17] J. Park, C. Spånslätt, Y. Gefen, and A. D. Mirlin, Noise on the non-abelian  $\nu = 5/2$  fractional quantum hall edge, *Phys. Rev. Lett.* **125**, 157702 (2020).
- [18] S. Manna, A. Das, M. Goldstein, and Y. Gefen, Full classification of transport on an equilibrated  $5/2$  edge via shot noise, [arXiv:2212.05732](https://arxiv.org/abs/2212.05732) (2022).
- [19] C. Nosiaglia, J. Park, B. Rosenow, and Y. Gefen, Incoherent transport on the  $\nu = 2/3$  quantum hall edge, *Phys. Rev. B* **98**, 115408 (2018).
- [20] C. Spånslätt, J. Park, Y. Gefen, and A. D. Mirlin, Conductance plateaus and shot noise in fractional quantum hall point contacts, *Phys. Rev. B* **101**, 075308 (2020).
- [21] C. Spånslätt, Y. Gefen, I. V. Gornyi, and D. G. Polyakov, Contacts, equilibration, and interactions in fractional quantum hall edge transport, *Phys. Rev. B* **104**, 115416 (2021).
- [22] J. Park, B. Rosenow, and Y. Gefen, Symmetry-related transport on a fractional quantum hall edge, *Phys. Rev. Res.* **3**, 023083 (2021).
- [23] S. Biswas, R. Bhattacharyya, H. K. Kundu, A. Das, M. Heiblum, V. Umansky, M. Goldstein, and Y. Gefen, Shot noise does not always provide the quasiparticle charge, *Nature Physics* **18**, 1476 (2022).
- [24] A. Bid, N. Ofek, H. Inoue, M. Heiblum, C. L. Kane, V. Umansky, and D. Mahalu, Observation of neutral modes in the fractional quantum hall regime, *Nature* **466**, 585 (2010).
- [25] R. Bhattacharyya, M. Banerjee, M. Heiblum, D. Mahalu, and V. Umansky, Melting of interference in the fractional quantum hall effect: Appearance of neutral modes, *Phys. Rev. Lett.* **122**, 246801 (2019).
- [26] S. K. Srivastav, R. Kumar, C. Spånslätt, K. Watanabe, T. Taniguchi, A. D. Mirlin, Y. Gefen, and A. Das, Vanishing thermal equilibration for hole-conjugate fractional quantum hall states in graphene, *Phys. Rev. Lett.* **126**, 216803 (2021).
- [27] R. A. Melcer, B. Dutta, C. Spånslätt, J. Park, A. D. Mirlin, and V. Umansky, Absent thermal equilibration on fractional quantum hall edges over macroscopic scale, *Nature Communications* **13**, 1 (2022).
- [28] R. Kumar, S. K. Srivastav, C. Spånslätt, K. Watanabe, T. Taniguchi, Y. Gefen, A. D. Mirlin, and A. Das, Observation of ballistic upstream modes at fractional quantum hall edges of graphene, *Nature Communications* **13**, 1 (2022).
- [29] We define the time average of an operator  $x$  as  $\langle x \rangle = \lim_{\tau \rightarrow \infty} \frac{1}{\tau} \int_{-\tau}^{\tau} x(t) dt$ .
- [30] J. Nakamura, S. Liang, G. C. Gardner, and M. J. Manfra, Half-integer conductance plateau at the  $\nu = 2/3$  fractional quantum hall state in a quantum point contact, *Phys. Rev. Lett.* **130**, 076205 (2023).
- [31] S. Manna, A. Das, and M. Goldstein, Shot noise as a diagnostic in the fractional quantum hall edge zoo, [arXiv:2307.05173](https://arxiv.org/abs/2307.05173) (2023).
- [32] S. Manna, A. Das, and M. Goldstein, Shot noise classification of different conductance plateaus in a quantum point contact at the  $\nu = 2/3$  edge, [arXiv:2307.05175](https://arxiv.org/abs/2307.05175) (2023).
- [33] M. Banerjee, M. Heiblum, V. Umansky, D. E. Feldman, Y. Oreg, and A. Stern, Observation of half-integer ther-

- mal hall conductance, *Nature* **559**, 205 (2018).
- [34] A. Aharon-Steinberg, Y. Oreg, and A. Stern, Phenomenological theory of heat transport in the fractional quantum hall effect, *Phys. Rev. B* **99**, 041302 (2019).
- [35] N. Read and E. Rezayi, Beyond paired quantum hall states: Parafermions and incompressible states in the first excited landau level, *Phys. Rev. B* **59**, 8084 (1999).
- [36] M. Yutushui and D. F. Mross, Identifying non-abelian anyons with upstream noise, [arXiv:2305.14422](https://arxiv.org/abs/2305.14422) (2023).
- [37] S. Biswas, H. K. Kundu, V. Umansky, and M. Heiblum, Electron pairing of interfering interface-based edge modes, [arXiv:2304.05140](https://arxiv.org/abs/2304.05140) (2023).
- [38] Y. Ronen, T. Werkmeister, D. H. Najafabadi, A. T. Pierce, L. E. Anderson, Y. J. Shin, S. Y. Lee, Y. H. Lee, B. Johnson, K. Watanabe, T. Taniguchi, A. Yacoby, and P. Kim, Aharonov–bohm effect in graphene-based fabry–pérot quantum hall interferometers, *Nature Nanotechnology* **16**, 563 (2021).
- [39] A. K. Paul, M. R. Sahu, K. Watanabe, T. Taniguchi, J. K. Jain, G. Murthy, and A. Das, Electrically switchable tunneling across a graphene pn junction: evidence for canted antiferromagnetic phase in  $\nu = 0$  state, [arXiv:2205.00710](https://arxiv.org/abs/2205.00710) (2022).
- [40] J. Wang, Y. Meir, and Y. Gefen, Spontaneous breakdown of topological protection in two dimensions, *Phys. Rev. Lett.* **118**, 046801 (2017).
- [41] N. John, A. D. Maestro, and B. Rosenow, Robustness of helical edge states under edge reconstruction, *Europhysics Letters* **140**, 26002 (2022).
- [42] A. Kitaev, Anyons in an exactly solved model and beyond, *Annals of Physics* **321**, 2 (2006).
- [43] A. Banerjee, C. A. Bridges, J. Q. Yan, A. A. Aczel, L. Li, M. B. Stone, G. E. Granroth, M. D. Lumsden, Y. Yiu, J. Knolle, S. Bhattacharjee, D. L. Kovrizhin, R. Moessner, D. A. Tennant, D. G. Mandrus, and S. E. Nagler, Proximate kitaev quantum spin liquid behaviour in a honeycomb magnet, *Nature Materials* **15**, 733 (2016).
- [44] Y. Kasahara, T. Ohnishi, Y. Mizukami, O. Tanaka, S. Ma, K. Sugii, N. Kurita, H. Tanaka, J. Nasu, Y. Motome, T. Shibauchi, and Y. Matsuda, Majorana quantization and half-integer thermal quantum hall effect in a kitaev spin liquid, *Nature* **559**, 227 (2018).
- [45] N. Batra and D. E. Feldman, Different fractional charges from auto- and cross-correlation noise in quantum hall states without upstream modes, [arXiv:2307.03713](https://arxiv.org/abs/2307.03713) (2023).